

PAPER

Carrier-mediated magnetism in transition metal doped Bi_2Se_3 topological insulator

To cite this article: Tome M Schmidt *et al* 2013 *J. Phys.: Condens. Matter* **25** 445003

View the [article online](#) for updates and enhancements.

You may also like

- [Study of the structural, electric and magnetic properties of Mn-doped \$\text{Bi}_2\text{Te}_3\$ single crystals](#)

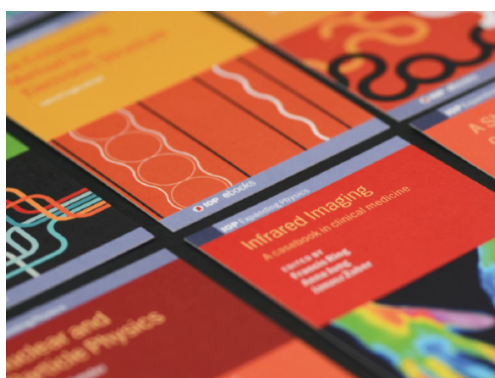
M D Watson, L J Collins-McIntyre, L R Shelford *et al.*

- [Enhanced photocatalytic properties of \$\text{Bi}_4\text{O}_7\text{Br}_2\$ by Mn doping: a first principles study](#)

Weibin Zhang, Shanjun Chen, Meilin He *et al.*

- [Microscopic position and structure of a shock in CA 184](#)

V Belitsky and G M Schütz



IOP | ebooks™

Bringing together innovative digital publishing with leading authors from the global scientific community.

Start exploring the collection—download the first chapter of every title for free.

Carrier-mediated magnetism in transition metal doped Bi_2Se_3 topological insulator

Tome M Schmidt¹, R H Miwa¹ and A Fazzio²

¹ Instituto de Física, Universidade Federal de Uberlândia, Caixa Postal 593, CEP 38400-902, Uberlândia, Minas Gerais, Brazil

² Instituto de Física, Universidade de São Paulo, CP 66318, 05315-970, São Paulo, SP, Brazil

E-mail: tschmidt@infis.ufu.br

Received 24 May 2013, in final form 2 August 2013

Published 20 September 2013

Online at stacks.iop.org/JPhysCM/25/445003

Abstract

The Dirac surface states of topological insulators are protected by time-reversal symmetry, suppressing backscattering. Magnetic impurities adsorbed on the surface of topological insulators are expected to degrade the coherence of these protected surface states, breaking time-reversal symmetry. Some results are in agreement with this prediction. There are others where no bandgap opening was observed. Here, based upon first principles calculations, we show that one mechanism that plays a key role in these controversial results is the intrinsic carrier concentration. The magnetic phase of Fe-, Co- and Ni-doped Bi_2Se_3 has been computed and compared to the same systems in the presence of n- or p-type doping. Our results show that the magnetic phase is dependent on both the carrier concentration and the magnetic impurity coverage, resulting in a phase diagram for the existence or not of the protected Dirac states.

(Some figures may appear in colour only in the online journal)

1. Introduction

The quantum matter phase of topological insulators (TIs), due to topological protection, exhibit spin texture and Dirac massless states, that allows spin currents without dissipation [1–4]. These properties open a number of opportunities for novel technologies, such as quantum computing, information processing, and spintronics. However, for practical applications it is necessary to dope those materials in a suitable way [5]. Usually, the undoped TIs Bi_2Se_3 and Bi_2Te_3 exhibit n-type character due to the presence of intrinsic defects. Currently, there is a general consensus that the presence of time-reversal invariant perturbation, like nonmagnetic impurities or defects, preserves the chiral spin texture of the topological surface states, and thus, the TI surface states are absent of backscattering channels. On the other hand, there is no such consensus for magnetic impurities lying on the TI surface.

Previous theoretical studies, based on effective Hamiltonian models [6–8], indicate the formation of a gapped system ruled by ordered magnetic moments oriented perpendicularly to the surface. This was verified through angle-resolved

photoemission spectroscopy (ARPES) experiments for Fe adatoms on the Bi_2Se_3 surface [5, 9]. The presence of magnetic impurities, like transition metal (TM), with the spin orientation out of the surface plane, breaks time-reversal symmetry (TRS), opening an energy gap at the Dirac point (DP), and gives rise to massive Dirac fermions. Those findings have been supported by our first principles calculations for Co impurities adsorbed on the Bi_2Se_3 surface [10], in agreement with a recent calculation for Ti and Co impurities [11]. The Co adatoms exhibit a ferromagnetic coupling with the net magnetic moment aligned perpendicularly to the Bi_2Se_3 surface. Similar net spin orientation has been verified for Fe adatoms lying on Bi_2Se_3 [12]. In striking contrast, very recent experimental results indicate that there is no energy gap at the DP, namely it has been preserved upon the presence of magnetic impurities on the Bi_2Se_3 and Bi_2Te_3 surfaces [13, 14]. Recent first principles investigations of moderate Mn-doped Bi_2Te_3 shows that TRS is broken, but surface states with spin texture similar to that of undoped system is preserved [15]. A combination of theory and experiment [16] shows that Fe adatoms on the Bi_2Se_3 surface exhibit a predominant in-plane magnetic orientation (70° with

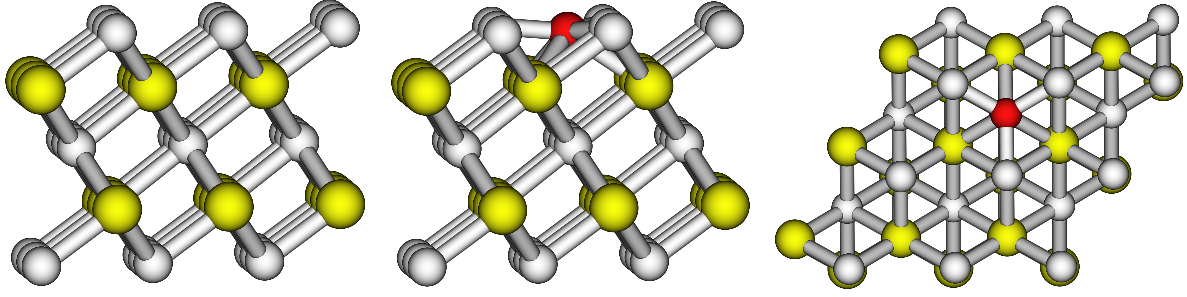


Figure 1. Left: side view of the first QL of Bi_2Se_3 structure. Middle and right: side and top view, respectively, of a QL containing one TM impurity. The biggest (yellow), the medium (gray), and the smaller (red) balls represent the Bi, Se and TM ion positions, respectively.

respect to the $\text{Bi}_2\text{Se}_3(111)$ direction), where an energy shift of the DP has been observed—however, the DP has been preserved. In contrast, first principles results for Cr and Fe substitutional at Bi site present a magnetic ground state perpendicular to the quintuple layers (QL) [17]. Lasia and Brey [18] showed that the magnetization is dependent on the temperature and slab thickness. They showed that at low temperatures the impurities order ferromagnetically, while by raising the temperature the system goes to a spin density wave phase. A systematic study of the energetic and electronic of TM-doped Bi_2Se_3 show that the magnetic orientation is not the same for different TMs at the same site [19]. More than that, the most stable site for the TMs are different when we change the valence of the TMs from Cr to Ni.

In this work we show that the energy gap at the DP and the chiral spin texture of TIs, adsorbed by magnetic impurities, can be tuned through n or p-type doping processes. We have considered the Bi_2Se_3 surface adsorbed by Fe ($\text{Fe}/\text{Bi}_2\text{Se}_3$), Co ($\text{Co}/\text{Bi}_2\text{Se}_3$), and Ni ($\text{Ni}/\text{Bi}_2\text{Se}_3$) TMs. Our results show that the excess electrons of the intrinsic doping can compensate the TM states, quenching the net magnetic moment, preserving the robustness of the massless Dirac cone.

2. Calculation method

We performed *ab initio* electronic structure calculations, using the density functional theory (DFT) within the generalized gradient approximation (GGA) for the exchange and correlation potential [20]. The spin–orbit interaction was self-consistently treated by using the fully relativistic pseudopotential within the projector augmented wave (PAW) method [21]. The Kohn–Sham (KS) equations are solved using the self-consistent method, as implemented in the Vienna *ab initio* package simulation (VASP) [22]. The KS orbitals are expanded in a plane wave basis set with an energy cutoff of 300 eV. The Brillouin zone was sampled, according to the Monkhorst–Pack [23] scheme, by using a number of k -points up to $8 \times 8 \times 3$, such that the total energy was converged. Although the Bi_2Se_3 crystallizes in the rhombohedral lattice, in our calculations we use a supercell with hexagonal lattice, because we want to simulate a surface, and we choose the van der Waals (111) surface, which presents hexagonal symmetry. A slab method has been used with a vacuum layer of at least 8 Å to avoid interactions

between adjacent surfaces. A slab thickness of 4 QLs have been used, keeping the experimental lattice parameter. This slab is enough to obtain the correct surface massless Dirac cone in agreement with other calculations [24], and in some agreement with experimental observations [25]. We have considered a number of hexagonal surface periodicities, namely 1×1 , 2×2 , 3×3 , in order to simulate different concentrations of Co adatoms on the Bi_2Se_3 surface. For Fe and Ni we considered only 2×2 periodicity. In figure 1 we plot the first QL of a 3×3 unit cell, free of defects and containing one TM impurity.

The n- or p-type doping concentrations have been simulated by adding or removing fraction of electrons from the system, respectively. The DFT calculation may underestimate the electronic correlations, especially for the TM impurities. So we include an on-site electron–electron interaction U (in the DFT + U approach) for the d orbitals. We change the on-site repulsion from $U = 1.0$ to 3.0 eV for Fe, Co and Ni impurities. The occupation of the TM d orbitals have been computed by performing a projection of the Kohn–Sham orbitals on spherical harmonics, which is then integrated inside a sphere centered at the TM doped ion site.

3. Results and comments

The most stable position for a TM metal on the surface of Bi_2Se_3 is at the fcc or hcp hollow. Actually the two positions are almost degenerated in energy, similarly as reported before [10, 16]. Our results show that isolated TMs adsorbed on the surface of TI effect a trend on the magnetization. The TM states hybridize with the TI, resulting in a net magnetic moment for Fe, Co and Ni around 3, 2 and 0 μ_B , respectively. The net magnetic moment is mostly ruled by the 3d orbitals of the adsorbed TMs, while the spin polarizations induced on the nearest-neighbor Bi (6p) and Se (4p) atoms are very small. For the three TM impurities the spin-up 3d levels are fully occupied. The spin-down 3d levels determine the magnetization. Without the inclusion of spin–orbit (SO) interactions $\text{Fe}/\text{Bi}_2\text{Se}_3$ exhibits a $3d^{7.7}$ electronic configuration, as can be seen in figure 2. This configuration occurs due to a s–d population inversion, similarly as observed by Ludwig and Woodbury [26] and explained by Fazzio *et al* [27] in II–VI semiconductors. This s–d transition occurs because the surface impurity hybridizes

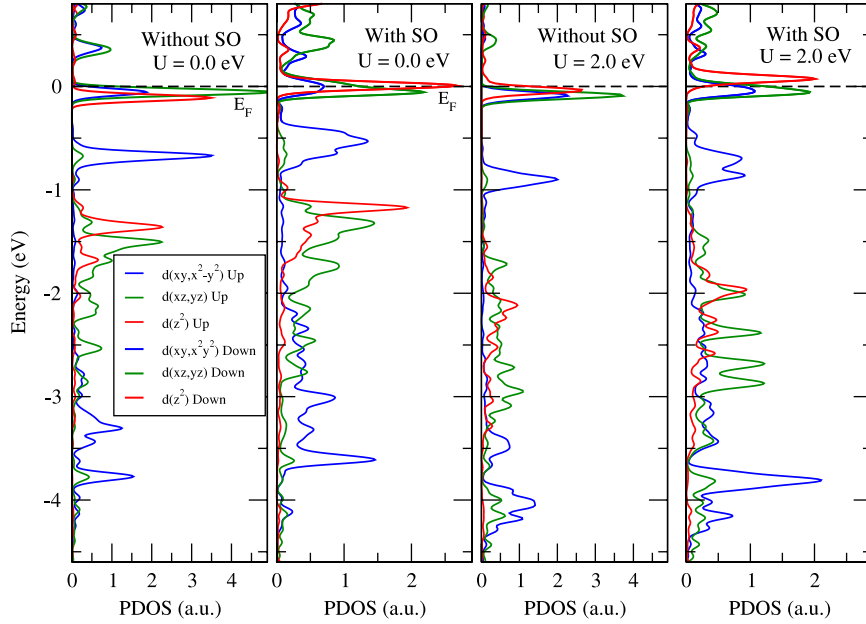


Figure 2. Projected density of states of Fe d orbitals, without and with SO interactions. Blue, green and red lines represent d_{xy, x^2-y^2} , $d_{xz, yz}$ and d_{z^2} orbitals, respectively. On the left we have the results without correction of Coulomb repulsion, and on the right we include an on-site repulsion $U = 2.0$ eV.

with the Bi_2Se_3 states, as can be seen in figure 2. By turning on the SO coupling, the d_{z^2} orbital is shifted toward the conduction band. This depopulation of the d_{z^2} orbital is due to the presence of occupied protected surface metallic bands, which appear only when SO coupling is presented. In this way the occupation for Fe is $3d^{6.9}$.

In order to check the importance of the U -Coulomb repulsion, we include an on-site $U = 1.0, 2.0$ and 3.0 eV. $U = 3.0$ eV has been used recently for Fe at Bi site in Bi_2Se_3 [17]. For $U = 1.0$ eV the changes on the energy levels of the Fe d orbitals do not alter the occupation. In figure 2, we can see that the most affected d orbitals are d_{z^2} and $d_{xz, yz}$, by including the U -Coulomb repulsion. By increasing the electronic repulsion to $U = 2.0$ eV we can see in this figure that the majority d_{z^2} orbital is shifted deeper inside the valence band, while the minority d_{z^2} is shifted toward the conduction band, when the SO interaction is included. The occupation of the d orbitals is now $3d^{6.8}$ and $3d^{7.0}$ for $U = 2.0$ and 3.0 eV, respectively.

Similarly for Co/ Bi_2Se_3 system, the majority spin levels are fully occupied, presenting a $3d^{8.1}$ occupation, by including on-site $U = 2.0$ eV repulsion and SO interaction. For Ni/ Bi_2Se_3 , both spin channels of Ni 3d orbitals are fully occupied, resulting in no net magnetization, even including on-site U -Coulomb correction. This d^{10} occupation for the Ni occurs because Ni presents a lower Coulomb interaction as reported in the literature [27], as compared to Co and Fe. For a small hybridization the s-d transition will take place and the d orbitals of the Ni will be fully occupied. The electronic U -Coulomb repulsion is not enough to induce a vacancy.

The TM ions raise the Fermi level, in such a way that the doped Bi_2Se_3 for the three TMs studied here become n-type systems, which is in agreement with experiments [5, 9, 13, 14]. This n-type doping can be understood by two

main factors: the s-d transition and the hybridization. The 4s orbitals of the TM turn unoccupied when adsorbed on the Bi_2Se_3 surface. But the 3d orbitals do not get the total s electrons, remaining partially charged in the hybridization, which induces n-type doping. The net magnetic moment due to Fe and Co adsorbed impurities are $\sim 100\%$ spin polarized aligned perpendicular to the TI surface, presenting a magnetic anisotropy energy around 6 meV, either for Fe [12], or Co impurity [10]. This out-of-plane easy axis is a consequence of the vacancy of the d_{z^2} orbital, which favor out-of-plane magnetic moment. The depopulation of the spin-down d_{z^2} orbital is more clear when on-site U -Coulomb correction is included (see figure 2). An out-of-plane orientation has also been obtained recently for Fe at Bi site in Bi_2Se_3 [17]. The presence of this magnetism, as already predicted [6, 28–30], breaks TRS, opening up a surface bandgap. On the other hand, if the magnetic moment is aligned in-plane, our first principles results confirm the preservation of the DP—only an energetic shifting on the Dirac crossing is obtained. Recent experimental results for low concentration of Fe adatoms on Bi_2Se_3 found a magnetic moment aligned almost in-plane, 70° with respect to the (111) direction [16]. These discrepancies between the theoretical prediction and the experiments may be better understood if we look at the Lasia and Brey results [18], where it was shown that the magnetization is dependent on the temperature and slab thickness. They showed that at low temperatures the impurities order ferromagnetically, while by raising the temperature the system goes to a spin density wave phase. Our first principles results for Ni impurity, where no net magnetization is presented, show that the massless Dirac cone is always preserved, and the Fermi level is above the Dirac crossing, resulting in an n-type doping.

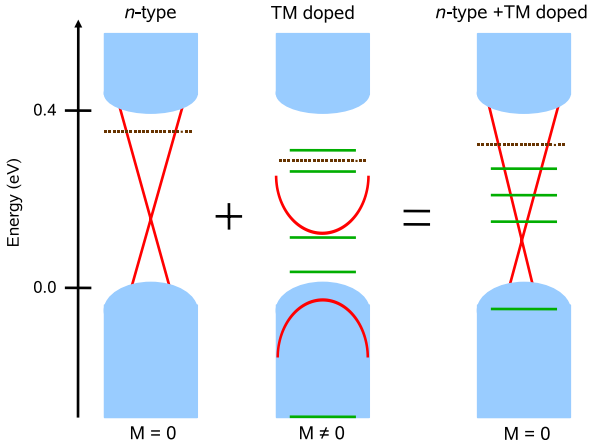


Figure 3. Evolution of the electronic structure when an n-type TI is doped with TM on the surface. The horizontal (green) solid lines represent the localized d orbitals of the TM impurities. The horizontal dashed lines are the Fermi levels for each separately calculated system. M denotes net magnetization.

In order to understand the effects of an n-type system on the TM-doped TI, initially we focus on the $\text{Co}/\text{Bi}_2\text{Se}_3$ system. The net magnetic moment $M \approx 2 \mu_B$ is ruled by empty 3d states lying just above the Fermi level. In this case, adding electrons to the highest unoccupied Co 3d levels, i.e. mediated by an n-type doping, the net magnetic moment is quenched ($M = 0$). As a consequence, the TRS is recovered, and the robust surface states are also recovered. Figure 3 summarizes

the magnetic moment quenching for the n-type $\text{Co}/\text{Bi}_2\text{Se}_3$, that is, we will have $M = 0$ by tuning the position of E_F (due to the n-type doping) with respect to the empty minority spin states of Co 3d. The helical spin texture of the TIs is recovered upon the quenching process. Figure 4 presents the spin density of state of n-type $\text{Co}/\text{Bi}_2\text{Se}_3$ with $M = 0$, where we find similar spin texture in comparison with the pristine Bi_2Se_3 system. The agreement between the Co-doped and pristine surfaces is more evident near the DP, while far from the DP there is a contribution from Co 3d to the calculated spin density of state. On the other hand, for neutral $\text{Co}/\text{Bi}_2\text{Se}_3$, without n-type doping, the in-plane spin texture is completely destroyed.

For the $\text{Fe}/\text{Bi}_2\text{Se}_3$ system, although the carrier (electron) concentration (due to n-type doping) is larger in comparison with $\text{Co}/\text{Bi}_2\text{Se}_3$, since (i) we have around three empty minority spin orbitals ($3d_{z^2}$ and $3d_{xy-x^2-y^2}$), and (ii) our band structure calculations indicate that those empty Fe 3d orbitals are resonant within the Bi_2Se_3 conduction band, figure 2, and the magnetic moment will also be quenched for a suitable n-doping. In (ii) most of the additional carriers will spread out within the conduction bands lying below the empty Fe 3d orbitals, until we have E_F above the empty 3d orbitals. Here it is worth to pointing out that the TM empty states are quite hybridized with host Bi_2Se_3 . Finally, the electronic structure of the $\text{Ni}/\text{Bi}_2\text{Se}_3$ system suggests that we may have a net magnetic moment by adding holes—p-type doping. In this case, we will have an empty minority 3d spin state, with $M \neq 0$, opening an energy gap at the DP. Indeed, this is what

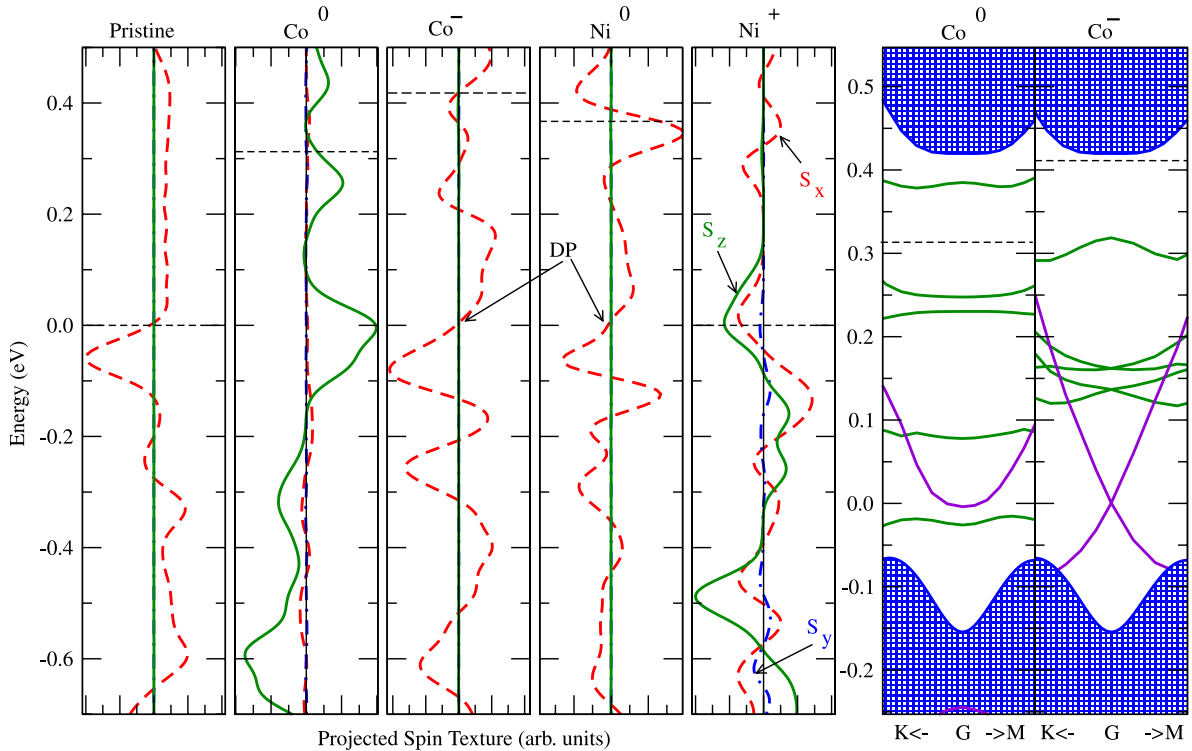


Figure 4. Spin density projected on each S_σ spin component for neutral and negative charged Co, and neutral and positive charged Ni doped Bi_2Se_3 . Also the pristine TI spin texture is shown. On the right the band structure of neutral and negative charged Co impurity is shown. The horizontal dashed line is the Fermi level position. The spin texture is computed along the Γ -M direction.

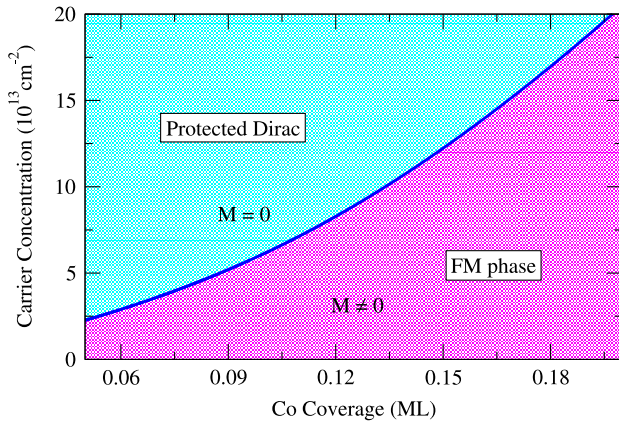


Figure 5. Phase diagram showing where the protected Dirac cone is preserved according to the carrier concentration and the TM Co coverage. The magnetization is zero when the Dirac cone is presented.

we find by performing an electronic band structure calculation for the positively charged Ni/Bi₂Se₃ system, resulting in a $M = 0.4 \mu_B$ and the helical spin texture being suppressed (see figure 4), whereas by adding electrons to the Ni/Bi₂Se₃ system, n-type doping, the DP has been preserved, since those extra electrons will be delocalized within the conduction band.

Those findings can explain why in some experiments with TM-doped TI preserves the Dirac cone [13, 14]. It is worth noting that there are other proposals aiming to explain the maintenance of the gapless DP upon the presence of magnetic impurities: for instance, the energetic preference for an in-plane magnetic moment for Fe adatoms on Bi₂Se₃, as suggested in [16]. Indeed, through magnetic anisotropy energy (MAE) calculations we find that Co atoms embedded between the QLs of Bi₂Se₃ exhibit an in-plane magnetic moment, while for Co adatoms on the Bi₂Se₃ surface our MAE results reveal an out-of-plane magnetic moment, opening an energy gap at the DP [10]. Similar MAE calculations performed for Fe adatoms lying on the Bi₂Se₃ surface also indicate an out-of-plane magnetization [12]. Recent investigations of magnetic impurities in Bi₂Se₃, as a function of the temperature, support an out-of-plane ferromagnetic order at low temperature [18]. Within this scenario, we can infer that a gapless DP in TIs doped with magnetic impurities can be ruled by (i) quenching mechanism through n- or p-type doping processes, and/or (ii) energetic preference for an in-plane magnetic moment for impurities lying on the TI surface.

Our proposed quenching mechanism presents a dependence between the concentrations of n-type carriers and the adsorbed TMs. That is, if the n-type carrier concentration is not enough to compensate the empty TM d states, we will have $M \neq 0$, and thus an energy gap is expected at the DP, with broken TRS. As showed in figure 5, where we present the results for Co-doped Bi₂Se₃, the system can be magnetic or nonmagnetic, depending on the n-type concentration and the Co coverage. The curve that separates the phases is an upper limit, since we do not vary continuously the concentration. Without the n-type doping, the Co impurity presents a net

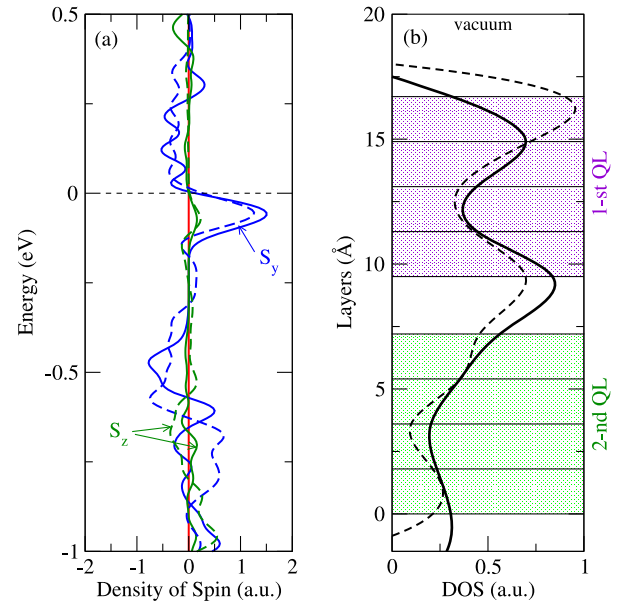


Figure 6. Projected spin density (a) and density of states for the surface Dirac cone (b) computed along the Γ -K direction. Dashed lines are the results for pristine Bi₂Se₃, and solid lines are for a system with a Se vacancy defect present.

magnetic moment, independent on the Co coverage. Figure 5 shows that there is an upper limit for the TM coverage to suppress the magnetic phase, avoiding backscattering, which is in agreement with the Valla *et al* experiments [14].

The origin of the n-type TI has been attributed to the presence of Se vacancies [9, 31], and more recently also the anti-site Se atom at Bi site defect has been proposed to be an intrinsic donor-like defect [32]. We investigate if the Se vacancy could change the conclusions described above. Among many positions for a Se vacancy in Bi₂Se₃, we find that the formation energy for a Se vacancy either on top of the TI or at the vdW interlayer spacings are the most stable positions, differing from each other by only a tenth of meV, in agreement with previous calculation [32]. The Se vacancy does not introduce any defect level inside the bulk bandgap. The perturbation on the electronic structure due to the presence of a Se vacancy defect on the surface or between the QLs of the TI is only detected on the Dirac states: the protected surface levels become more weakly bounded, increasing the Fermi level. The spin texture of the Dirac states is well preserved when a vacancy is presented in the system, which also is in agreement with experiments. As we can see in figure 6(a) the pristine (dashed lines) spin density projected for each spin component is very similar to that with a Se vacancy in the system. Another interesting finding is that the vacancy defect shifts the protected surface states inside the crystal. We can see in figure 6(b) that the density of states of the topological Dirac cone for pristine Bi₂Se₃ is mostly localized on the top surface Se atoms (solid line), in agreement with other results [33]. On the other hand, for a vacancy defect part of the density of states is shifted to Se atoms deeper inside the crystal (dashed line). The Dirac cone states are now more localized in the Se atoms positioned between the first

and second QLs. The result of this shifting is a less bounded protected surface state, increasing the Fermi level.

4. Summary

In summary, using first principles calculations, we investigate the robustness of the topological protected surface states against magnetic impurities. Using on-site correction for the Coulomb repulsion, we determine the energies of the TM 3d states with respect to the bulk bandgap and the surface Dirac crossing. We show that the magnetic stability of TM adsorbed on the Bi₂Se₃ surface is dependent on the carrier concentration and the magnetic impurity coverage. Magnetic impurities adsorbed on the TI surface that introduce partially occupied 3d levels around the bulk bandgap originate a net magnetic moment. These 3d open-shell impurities break TRS, opening up a surface bandgap. By varying the carrier concentration, the 3d states can become occupied, quenching the net magnetic moment, preserving the topological protected surface states. More than that, we show that the spin texture of these coherent protected Dirac-like states are quite similar to those of defect-free TI.

The existence or not of the protected Dirac states can be governed by a phase diagram of the carrier concentration versus magnetic impurity coverage. This transition from a topological protected state to a trivial phase helps us to understand why in some experiments the Dirac states are preserved, while in others they are not. Our results also demonstrate that TM-doped TIs can be an interesting system for spintronic applications.

Acknowledgments

This work was supported by the Brazilian agencies FAPEMIG, FAPESP, CAPES, and CNPq.

References

- [1] Fu L, Kane C L and Mele E J 2007 *Phys. Rev. Lett.* **98** 106803
- [2] Hsieh D, Qian D, Wray L, Xia Y, Hor Y, Cava R J and Hasan M Z 2008 *Nature* **452** 970
- [3] Zhang H, Liu C-X, Qi X-L, Dai X, Fang Z and Zhang S-C 2009 *Nature Phys.* **5** 438
- [4] Hsieh D *et al* 2009 *Science* **323** 919
- [5] Chen Y L *et al* 2010 *Science* **329** 659
- [6] Liu Q, Liu C-X, Xu C, Qi X-L and Zhang S-C 2009 *Phys. Rev. Lett.* **102** 156603
- [7] Zhou X, Fang C, Tsai W-F and Hu J P 2009 *Phys. Rev. B* **80** 245317
- [8] Guo H-M and Franz M 2010 *Phys. Rev. B* **81** 041102(R)
- [9] Wray L A, Xu S-Y, Xia Y, Hsieh D, Fedorov A V, Hor Y S, Cava R J, Bansil A, Lin H and Hasan M Z 2011 *Nature Phys.* **7** 32
- [10] Schmidt T M, Miwa R H and Fazzio A 2011 *Phys. Rev. B* **84** 245418
- [11] Jin K-H and Jhi S-H 2012 *J. Phys.: Condens. Matter* **24** 175001
- [12] Li Z L, Yang J H, Chen G H, Whangbo M-H, Xiang H J and Gong X G 2012 *Phys. Rev. B* **85** 054426
- [13] Scholz M R, Sánchez-Barriga J, Marchenko D, Varykhalov A, Volykhov A, Yashina L V and Rader O 2012 *Phys. Rev. Lett.* **108** 256810
- [14] Valla T, Pan Z-H, Gardner D, Lee Y S and Chu S 2012 *Phys. Rev. Lett.* **108** 117601
- [15] Henk J, Ernst A, Ereemeev S V, Chulkov E V, Maznichenko I V and Mertig I 2012 *Phys. Rev. Lett.* **108** 206801
- [16] Honolka J *et al* 2012 *Phys. Rev. Lett.* **108** 256811
- [17] Zhang J-M, Zhu W, Zhang Y, Xiao D and Yao Y 2012 *Phys. Rev. Lett.* **109** 266405
- [18] Lasia M and Brey L 2012 *Phys. Rev. B* **86** 045317
- [19] Abdalla L B, Seixas L, Schmidt T M, Miwa R H and Fazzio A 2013 *Phys. Rev. B* **88** 045312
- [20] Perdew J P, Burke K and Ernzerhof M 1996 *Phys. Rev. Lett.* **77** 3865
- [21] Blöchl P E 1994 *Phys. Rev. B* **50** 17953
- [22] Kresse G and Furthmüller J 1996 *Phys. Rev. B* **54** 11169
- [23] Monkhorst H J and Pack J D 1976 *Phys. Rev. B* **13** 5188
- [24] Yazyev O V, Moore J E and Louie S G 2010 *Phys. Rev. Lett.* **105** 266806
- [25] Zhang Y *et al* 2010 *Nature Phys.* **6** 584
- [26] Ludwig G W and Woodbury H H 1962 *Solid State Phys.* **13** 223
- [27] Fazzio A, Caldas M J and Zunger A 1984 *Phys. Rev. B* **30** 3430
- [28] Biswas R R and Balatsky A V 2010 *Phys. Rev. B* **81** 233405
- [29] Zhu J-J, Yao D-X, Zhang S-C and Chang K 2011 *Phys. Rev. Lett.* **106** 097201
- [30] Abanin D A and Pesin D A 2011 *Phys. Rev. Lett.* **106** 136802
- [31] Hsieh D *et al* 2009 *Nature* **460** 1101
- [32] Scanlon O, King P D C, Singh R P, de la Torre A, Walker S M, Balakrishnan G, Baumberger F and Catlow C R A 2012 *Adv. Mater.* **24** 00187
- [33] Zhang W, Yu R, Zhang H-J, Dai X and Fang Z 2010 *New J. Phys.* **12** 065013